

Non-peripherally octaalkyl-substituted nickel phthalocyanines used as non-dopant hole transport materials in perovskite solar cells

Fei Qi(齐飞), Bo Wu(吴波), Junyuan Xu(徐俊源), Qian Chen(陈潜), Haiquan Shan(单海权), Jiaju Xu(许家驹), and Zong-Xiang Xu(许宗祥)

Citation: Chin. Phys. B, 2021, 30 (**10**): 108801. DOI: 10.1088/1674-1056/ac1573
Journal homepage: http://cpb.iphy.ac.cn; http://iopscience.iop.org/cpb

What follows is a list of articles you may be interested in

Stabilization of formamidinium lead iodide perovskite precursor solution for blade-coating efficient carbon electrode perovskite solar cells

Yu Zhan(占宇), Weijie Chen(陈炜杰), Fu Yang(杨甫), and Yaowen Li(李耀文)
Chin. Phys. B, 2021, 30 (**8**): 088803. DOI: 10.1088/1674-1056/abfbcb

Improved efficiency and stability of perovskite solar cells with molecular ameliorating of ZnO nanorod/perovskite interface and Mg-doping ZnO

Zhenyun Zhang(张振雲), Lei Xu(许磊), and Junjie Qi(齐俊杰)
Chin. Phys. B, 2021, 30 (**3**): 038801. DOI: 10.1088/1674-1056/abd748

Highly efficient bifacial semitransparent perovskite solar cells based on molecular doping of CuSCN hole transport layer

Shixin Hou(侯世欣), Biao Shi(石标), Pengyang Wang(王鹏阳), Yucheng Li(李玉成), Jie Zhang(张杰), Peirun Chen(陈沛润), Bingbing Chen(陈兵兵), Fuhua Hou(侯福华), Qian Huang(黄茜), Yi Ding(丁毅), Yuelong Li(李跃龙), Dekun Zhang(张德坤), Shengzhi Xu(许盛之), Ying Zhao(赵颖), Xiaodan Zhang(张晓丹)
Chin. Phys. B, 2020, 29 (**7**): 078801. DOI: 10.1088/1674-1056/ab99ae

Two-step processed efficient perovskite solar cells via improving perovskite/PTAA interface using solvent engineering in PbI_2 precursor

Cao-Yu Long(龙操玉), Ning Wang(王宁), Ke-Qing Huang(黄可卿), Heng-Yue Li(李恒月), Biao Liu(刘标), Jun-Liang Yang(阳军亮)
Chin. Phys. B, 2020, 29 (**4**): 048801. DOI: 10.1088/1674-1056/ab7744

Effect of carrier mobility on performance of perovskite solar cells

Yi-Fan Gu(顾一帆), Hui-Jing Du(杜会静), Nan-Nan Li(李楠楠), Lei Yang(杨蕾), Chun-Yu Zhou(周春宇)
Chin. Phys. B, 2019, 28 (**4**): 048802. DOI: 10.1088/1674-1056/28/4/048802

Non-peripherally octaalkyl-substituted nickel phthalocyanines used as non-dopant hole transport materials in perovskite solar cells*

Fei Qi(齐飞)[1,2], Bo Wu(吴波)[1,2], Junyuan Xu(徐俊源)[1,2], Qian Chen(陈潜)[1,2], Haiquan Shan(单海权)[1,2], Jiaju Xu(许家驹)[1,2,†], and Zong-Xiang Xu(许宗祥)[1,2,‡]

[1] *Department of Chemistry, Southern University of Science and Technology, Shenzhen* 518000, *China*
[2] *Guangdong–Hong Kong–Macao Joint Laboratory for Photonic-Thermal-Electrical Energy Materials and Devices, Southern University of Science and Technology, Shenzhen* 518000, *China*

(Received 1 June 2021; revised manuscript received 28 June 2021; accepted manuscript online 18 July 2021)

This report presents two non-perihperally octaalkyl-substituted nickel phthalocyanines (NiPcs), namely, $NiEt_2Pc$ and $NiPr_2Pc$, for use as dopant-free hole transport materials in perovskite solar cells (PSCs). The length extension of the alkyl chains from ethyl to propyl significantly tunes the NiPcs' energy levels, thus reducing charge carrier recombination at the perovskite/hole transport layer (HTL) interface and leading to higher open-circuit voltage (V_{OC}) and short-circuit current density (J_{SC}) observed for the $NiPr_2Pc$-based PSC. And higher charge carrier mobility, higher thin film crystallinity, and lower surface roughness of the $NiPr_2Pc$ HTL compared with that of the $NiEt_2Pc$ one also lead to higher J_{SC} and fill factor (FF) observed for the $NiPr_2Pc$-based device. Consequently, the $NiPr_2Pc$-based PSC exhibits a higher power conversion efficiency (PCE) of 14.07% than that of the $NiEt_2Pc$-based device (8.63%).

Keywords: perovskite solar cells, metal phthalocyanines, hole transport layers

PACS: 88.40.hj, 73.40.–c, 81.20.–n **DOI:** 10.1088/1674-1056/ac1573

1. Introduction

Hybrid organicinorganic perovskites solar cells (PSCs) have drawn consideration attention due to the potential of achieving even higher efficiencies and low fabrication cost.[1–3] In the last decade, the power conversion efficiencies (PCEs) of the PSCs increased rapidly from 3.8% in 2009[4] to a certified 25.5% in 2020,[5] making this new photovoltaic technology more and more commercially attractive. As a necessary part of PSCs, hole transport layers (HTLs) play a vital role in enhancing hole extraction and transport, reducing charge carrier recombination, and protecting the perovskite layer from the moisture invasion, which is of great importance to obtain a PSC with high efficiency and good stability.[1,6–9] Current hole transport materials (HTMs) can be generally classified into three categories, including inorganic, polymeric, and small-molecule HTMs.[8] Among these, small-molecule HTMs are regarded as one of the most promising candidates owing to low-cost synthesis and easy chemical modification,[8] which is beneficial for mass manufacture. So far, spiro-OMeTAD (2,2',7,7'-Tetrakis[N,N-di(4-methoxyphenyl)amino]-9,9'-spirobifluorene) is one of most widely used small-molecule HTMs, and the highest PCE of 23.32% has been achieved.[10] However, the expensive preparation limits its commercialization. Further, due to the inherently low conductivity of the pristine spiro-OMeTAD, hydrophilic additives such as lithium bis(trifluoromethanesulfonyl)imide (LiTFSI), 4-tert–butyl pyridine (TBP), and so on, are usually necessary in order to improve the HTL conductivity, which induces poor device stability in air.[9,11,12]

As one class of small-molecule HTMs, organometallic compounds that contain a delocalized 18 π-electron conjugated system with a metal ion located at the central cavity, have also attracted considerable research attentions and efforts in recent years due to their excellent hole extraction and transport ability when employed as HTMs in PSCs.[8,9,11–14] So far, metal phthalocyanines (MPcs) are one of the most widely studied organometallic HTMs in PSCs.[15] This class of HTMs could be an ideal alternative to the expensive spiro-OMeTAD due to simple synthesis and easy purification,[8,9,16] as well as superior semiconducting nature originating from the interaction between organic ligand and central metal.[17] Also, the easy chemical modifications *via* varying central metal ions or introducing suitable functional groups to the π-conjugated cores may help to systematically adjust the chemical, physical, electronic, optical, and electronic properties of the compounds, therefore affording a suitable energy alignment with different perovskite active layers, facilitating charge extraction, and transfer, and allowing cost-effective solution-processed film preparation.[8,16] Moreover, MPcs can be used for fabricating HTLs without any dopant, which may help to lower fabrication cost and improve device stability.[1,8] It has

*Project supported by the Shenzhen Overseas High-level Talents Innovation Plan of Technical Innovation (Grant No. KQJSCX20180323140712012) and the Major Program of Guangdong Basic and Applied Research (Grant No. 2019B121205001).

†Corresponding author. E-mail: xujj@sustech.edu.cn
‡Corresponding author. E-mail: xuzx@sustech.edu.cn

© 2021 Chinese Physical Society and IOP Publishing Ltd

been reported that the PCE as high as 19.7% was obtained by using an arylamine-substituted copper phthalocyanine as non-dopant HTM.[16]

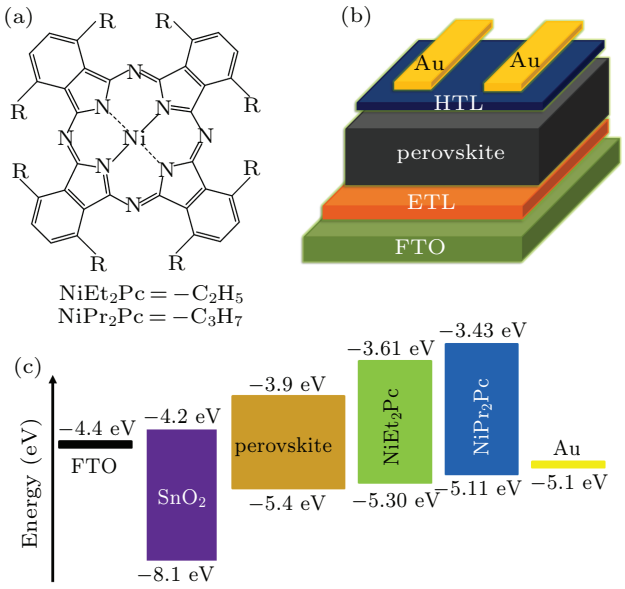


Fig. 1. (a) Chemical structures of the $NiEt_2Pc$ and $NiPr_2Pc$, (b) the device configuration, and (c) energy level diagrams of PSCs studied in this work.

The incorporation of substituents to the primary MPc skeleton is well known to be an effective strategy for MPcs' chemical modification.[1,15,18–21] The attached substituents bring their own special chemical and electronic characteristics to the MPc chromophores, thus significantly affecting the properties of the MPcs.[22] Particularly, MPcs functionalized with alkyl substituents on phenyl rings are of intensive interest during the last decade,[1,9,15,21,23–25] which not only increases the MPcs' solubility in common organic solvents, but also leads to higher charge carrier mobility due to shorter intermolecular π–π distance arising from the driving force of alkyl chains.[9,19] Also, alkyl groups increase hydrophobic nature of thin films, which would be more beneficial for the impedance of moisture ingress.[9,15] On the other hand, substitution positions at MPc ring may also play an important role in the properties that the MPc compound possess[22,26] Since a typical MPc molecule is composed of four isoindole moieties linked by a ring of nitrogen atoms[27] there are two positions available at the phenyl rings, to which substituents can be incorporated, namely peripheral position (2, 3, 9, 10, 16, 17, 23, 24) and non-peripheral position (1, 4, 8, 11, 15, 18, 22, 25).[28] The substitutions at different positions have been found to significantly affect the intrinsic properties of the MPc compounds, including optical, electronic and chemical properties, as well as aggregation behavior in solid state.[28] So far, the strategy of alkyl modification on MPcs for use as HTMs in PSCs mainly focuses on peripheral substitutions,[1,9,15,29,30] while non-peripheral substitutions are still rarely studied. With this in mind, we herein introduce two non-peripherally alky-substituted nickel phthalocyanines ($NiEt_2Pc$ and $NiPr_2Pc$, Fig. 1(a)) for use as non-dopant HTMs in PSCs. The solar cells based on these two MPcs have been fabricated and characterized, and the influence of alkyl chains on the device performances was then examined.

2. Experimental details

2.1. Materials

All the chemicals were purchased from the commercial sources and used without any further purification. The $NiEt_2Pc$ and $NiPr_2Pc$ utilized in this study were synthesized and purified according to similar method described in the reported literature,[26] involving a one-step synthesis from the starting materials of 36-diethylphthalonitrile and 36-dipropylphthalonitrile, respectively. The final products were further purified *via* vacuum sublimation in a tube-type heating furnace (Technol VDS-80) in order to fulfill the requirements of electronic applications. $NiEt_2Pc$: yield, 18%; MALDI-TOF MS m/z (M^+): calcd. for $[C_{48}H_{48}Ni_8Ni]^+$: 794.34; found: 794.30. UV-vis (chlorobenzene): $\lambda_{max} = 697$, 628 nm (Q-band). FTIR (KBr): $\nu = 2960$, 2928, 2866, 1605, 1573, 1515, 1450, 1405, 1341, 1177, 1091, 1054, 984, 916, 829, 759 cm^{-1}. $NiPr_2Pc$: yield, 16%; MALDI-TOF MS m/z (M^+): calcd. for $[C_{56}H_{64}Ni_8Ni]^+$: 906.46; found: 906.27. UV-vis (Dichloromethane): $\lambda_{max} = 699$, 630 nm (Q-band). FTIR (KBr): $\nu = 2954$, 2929, 2870, 1604, 1571, 1514, 1456, 1375, 1330, 1184, 1089, 985, 929, 819, 761 cm^{-1}.

2.2. Device fabrication and characterization

The n–i–p perovskites solar cells with the configuration of FTO/SnO_2/perovskite/$NiEt_2Py$ (or $NiPr_2Pc$)/Au (Fig. 1(b)) were fabricated and tested by the reported method[26] $CH_3NH_3PbI_3$ ($MAPbI_3$) was used as perovskite layer, and vacuum-deposited $NiEt_2Pc$ and $NiPr_2Pc$ layers as non-dopant HTLs.

3. Results and discussion

Thermogravimetric analysis was performed to investigate the thermal stability of the studied materials, as illustrated in Figs. 2(a) and 2(b). It can be found that both the $NiEt_2Pc$ and $NiPr_2Pc$ are thermally stable, and the decomposition temperatures, at which a 5% weight loss occurs, are estimated to be 437 °C and 446 °C, respectively, suggesting that the materials used this study are suitable HTMs in PSCs.

The ultraviolet-visible (UV-vis) absorption spectra of the $NiEt_2Pc$ and $NiPr_2Pc$ thin films deposition on fluorine-doped tin oxide (FTO) substrates are depicted in Figs. 3(a) and 3(b). Both the samples illustrate two strong characteristic absorption bands: one in the near UV region, known as B-band absorption, and another in the range of ca. 600 nm–800 nm,

known as Q-band absorption, which is the typical absorption behavior of the MPcs in solid state.[18] The B-band absorption is induced by $\pi \rightarrow \pi^*$ transition ($a_{2u} \rightarrow e^*_{1g}$) from the highest occupied molecular orbital (HOMO) to the lowest unoccupied molecular orbital (LUMO), and the Q-band absorption is due to $\pi \rightarrow \pi^*$ transition ($a_{1u} \rightarrow e^*_{1g}$) from HOMO to LUMO of the MPc ring.[1,9,30] The optical bandgaps of the $NiEt_2Pc$ and $NiPr_2Pc$ samples were determined from the absorption onsets and calculated to be 1.69 eV and 1.68 eV, respectively.

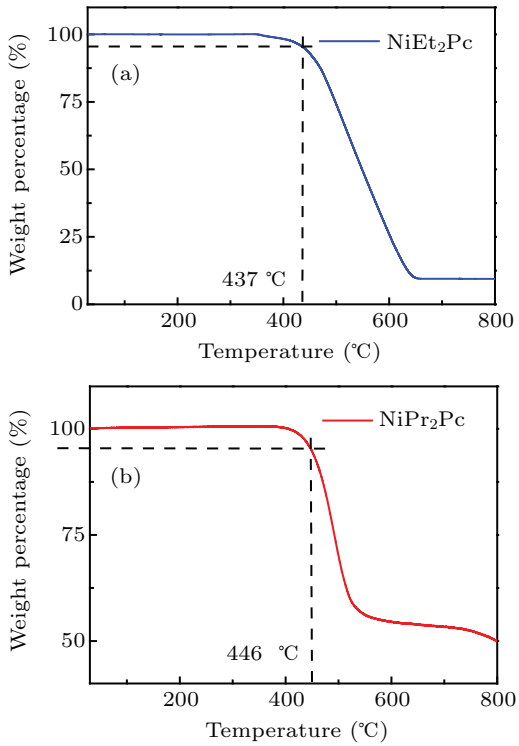


Fig. 2. Thermogravimetric analysis curves of (a) $NiEt_2Pc$ and (b) $NiPr_2Pc$.

The ionization energy measurement system (IPS-4) was employed to test the HOMO levels of the studied materials, as shown in Figs. 3(c) and 3(d). The HOMO level of the $NiEt_2Pc$ was found to be −5.30 eV, and with the length extension of alkyl chains from ethyl to propyl, a higher HOMO level is observed for the $NiPr_2Pc$ (5.11 eV). Using the optical bandgaps, the LUMO levels of the $NiEt_2Pc$ and $NiPr_2Pc$ were estimated to be −3.61 eV and −3.43 eV, respectively. The energy band diagram of the PSCs studied in this work is depicted in Fig. 1(c). It can be found that both the HOMO levels of the $NiEt_2Pc$ and $NiPr_2Pc$ are higher than the valence band (VB) of the $CH_3NH_3PbI_3$ absorber (−5.40 eV), which may help to provide sufficient driving forces for hole injection from the perovskite layer into the HTLs.[1,31] Also, the HOMO levels of the $NiEt_2Pc$ and $NiPr_2Pc$ are lower than the work function of the Au (−5.1 eV), which is favorable for hole collection on the Au electrode.[15] Furthermore, the $NiPr_2Pc$ exhibits a higher LUMO level than that of the $NiEt_2Pc$, which is more beneficial for blocking electron migration from the perovskite into the HTL, and thus reducing the opportunity for charge carrier recombination at the interface and within the HTL.[1]

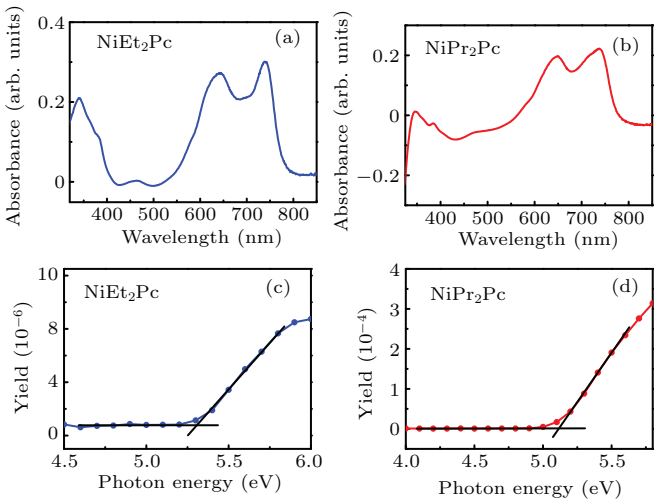


Fig. 3. (a), (b) UV-vis absorption spectra of the $NiEt_2Pc$ and $NiPr_2Pc$ thin films deposited on FTO with the thickness of 60 nm. (c), (d) The photoelectron yield spectroscopy (IPS-4) of the $NiEt_2Pc$ and the $NiPr_2Pc$.

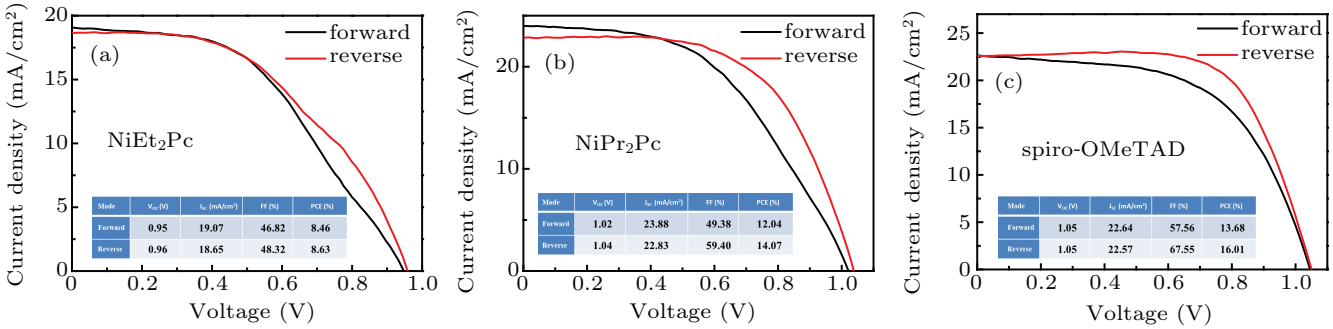


Fig. 4. *J*–*V* characteristics of best PSCs based on (a) $NiEt_2Pc$, (b) $NiPr_2Pc$, and (c) spiro-OMeTAD (doped) HTMs.

The PSCs using $NiEt_2Pc$ and $NiPr_2Pc$ HTLs were fabricated with the conventional n–i–p planar device configuration of FTO/SnO_2/perovskite/$NiEt_2Pc$ (or $NiPr_2Pc$)/Au, and the standard PSC using doped spiro-OMeTAD as HTL with the same configuration was also fabricated and characterized for reference according to the method described in the literature[26] The PSCs were characterized under a xenon lamp with AM 1.5, 100 mW/cm^2 simulated light illumination. The current–voltage (*J*–*V*) characteristics of the best devices are depicted in Fig. 4, and the relevant parameters such as the

open-circuit voltage (V_{OC}), short-circuit current density (J_{SC}), fill factor (FF), and PCE are summarized in the inset table. For each type of PSCs, 10 devices were characterized and the statistics of the photovoltaic parameters are depicted in Fig. 5 and Table 1. The champion PSC based on $NiEt_2Pc$ exhibits a J_{SC} of 18.65 mA/cm^2, V_{OC} of 0.96 V, FF of 48.32%, and PCE of 8.63%, while the best PSC based on $NiPr_2Pc$ has a J_{SC} of 22.83 mA/cm^2, V_{OC} of 1.04 V, FF of 59.40%, and PCE of 14.07% (Fig. 4 and Table 1). Higher values in J_{SC}, V_{OC}, and FF can be observed for the $NiPr_2Pc$-based PSC, giving rise to its higher PCE and exhibiting better hole extraction and transfer ability of the $NiEt_2Pc$ layer.

Interestingly, as shown in Fig. 1(c), although the $NiEt_2Pc$ has a deeper HOMO level of −5.30 eV than that of the $NiPr_2Pc$ (−5.11 eV), the $NiPr_2Pc$-based PSC has been found to exhibit a higher V_{OC} of 1.04 V than that of the $NiEt_2Pc$-based device (0.96 V) (Fig. 4, Table 1). It is well known that the V_{OC} of PSCs is strongly affected by charge carrier recombination inside the perovskite layer and/or at the adjacent interfaces, and serious charge recombination typically results in significant V_{OC} loss.[32,33] As shown in Fig. 1(c), higher LUMO level of the $NiPr_2Pc$ (−3.43 eV) compared with that of the $NiEt_2Pc$ may help to block electron injection from the perovskite layer into the HTL, and thus reduce charge recombination at the perovskite/HTL interface more effectively, which is more useful for reducing the V_{OC} loss, and leads to higher V_{OC} observed for the $NiPr_2Pc$-based device. Also, reduced charge carrier recombination at the perovskite/HTL interface and within the HTL arising from higher LUMO level of the $NiPr_2Pc$ is thought to be one main reason responsible for the enhanced J_{SC} and FF observed for the $NiPr_2Pc$-based device.[1,31]

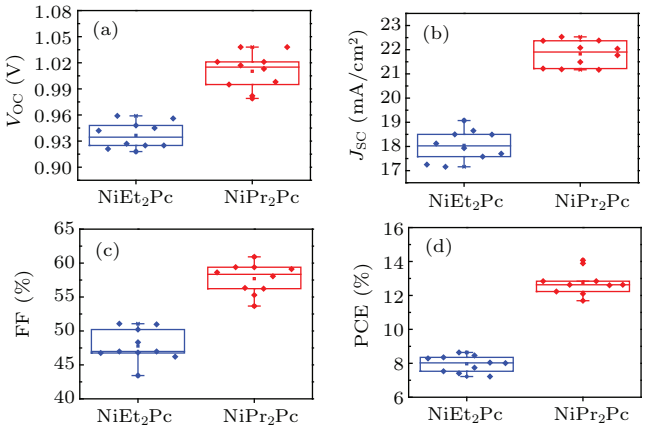


Fig. 5. Photovoltaic parameter statistics of the PSCs based on $NiEt_2Pc$ and $NiPr_2Pc$: (a) J_{SC}, (b) V_{OC}, (c) FF, and (d) PCE.

Table 1. Photovoltaic parameters of the PSCs based on $NiEt_2Pc$, $NiPr_2Pc$, and spiro-OMeTAD.

HTM	V_{OC} (V)	J_{SC} (mA/cm^2)	FF (%)	PCE[a] (%)
$NiEt_2Pc$	0.94±0.02 (0.96)	18.05±0.0.63 (18.65)	47.78±2.40 (48.32)	7.97±0.48 (8.63)
$NiPr_2Pc$	1.01±0.02 (1.04)	21.82±0.53 (22.83)	57.70±2.24 (59.40)	12.75±0.74 (14.07)
Spiro-OMeTAD[b]	1.05	22.57	67.55	16.01

[a]10 devices collected from the same batch; [b]spiro-OMeTAD doped with LiTFSI and TBP.

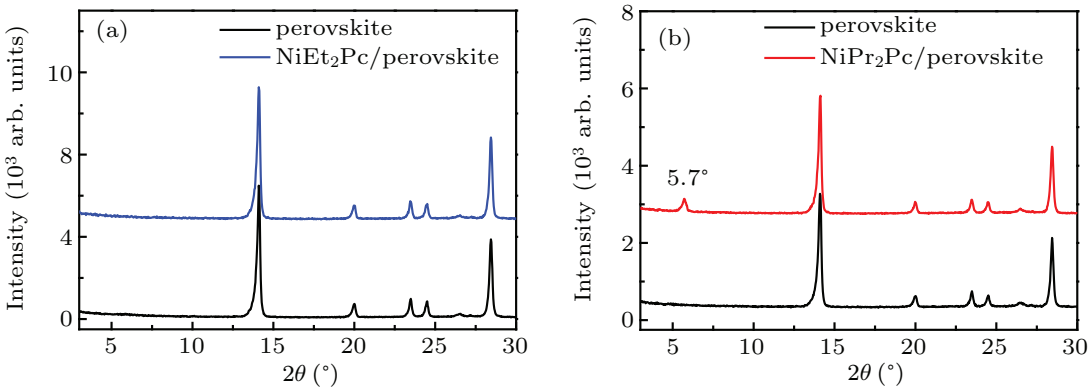


Fig. 6. GIXRD patterns of bare perovskite, (a) $NiEt_2Pc$/perovskite and (b) $NiPr_2Pc$/perovskite.

The film quality should be another factor that affects hole extraction and transfer ability of the HTLs. Thus grazing incidence x-ray diffraction (GIXRD) on two HTLs was examined to probe crystalline structures within the thin films. Figure 6 depicts the GIXRD patterns of the vacuum-deposited $NiEt_2Pc$ and $NiPr_2Pc$ thin films with the same thickness on top of the perovskite layer, and the GIXRD pattern of the bare perovskite layer was also characterized and presented for reference. As shown in Fig. 6(a), no obvious crystalline characteristic is observed for the $NiEt_2Pc$/perovskite sample, while the $NiPr_2Pc$/perovskite sample exhibits a diffraction signal with a 2θ value of 5.7° (Fig. 6(b)), indicating higher

thin film crystallinity as well as higher order of molecular arrangements within the thin film, which is more beneficial for hole extraction and transport, and thus leads to higher J_{SC} and FF found for the $NiPr_2Pc$-based PSC.[12] Atomic force microscopy (AFM) technologies were employed to study the morphologies of the HTLs, as illustrated in Fig. 7. The AFM image reveals that the bare perovskite layer exhibits the roughest surface morphology with a surface root-mean-square (RMS) roughness of 18.5 nm (Fig. 7(a)), while lower surface RMS roughness values are observed for the $NiEt_2Pc$ HTL (9.2 nm, Fig. 7(b)) and $NiPr_2Pc$ HTL (5.2 nm, Fig. 7(c)), which may help to provide better interface contact and form a more uniform conducting path for charge transfer.[1] The much lower surface RMS roughness observed for the $NiPr_2Pc$ HTL than that of the $NiEt_2Pc$ sample, which is more favorable for charge extraction and transfer, is considered to be another reason responsible for higher J_{SC} and FF of the device based on the $NiPr_2Pc$ HTL.

The hole transport properties of the $NiEt_2Pc$ and $NiPr_2Pc$ were investigated *via* bottom-contact field-effect transistor (FET) technology. The FETs using vacuum-deposited $NiEt_2Pc$ and $NiPr_2Pc$ thin films as active layers were fabricated according to the method described in the literature,[15] and the output and transfer characteristics of as-fabricated FETs are depicted in Fig. 8. Both the devices exhibits exhibit a p-type FET characteristic, with varying hole mobility values. The $NiEt_2Pc$-based FET exhibits a mobility of 1.33×10^{-5} $cm^2/V{\cdot}s$ and a threshold voltage of -14 V (Figs. 8(a) and 8(b)), which values are 3.64×10^{-4} $cm^2/V{\cdot}s$ and -4 V for the $NiPr_2Pc$-based device (Figs. 8(c) and 8(d)). The mobility of the $NiPr_2Pc$-based FET is one order of magnitude higher than that of the $NiEt_2Pc$-based one, clearly revealing that the length extension of alkyl chains from ethyl to propyl tunes the MPcs' hole transport properties effectively, which leads to better hole extraction of the $NiPr_2Pc$ HTL, and thus partly contributes to higher J_{SC} and FF values observed for the $NiPr_2Pc$-based PSC.[1,15]

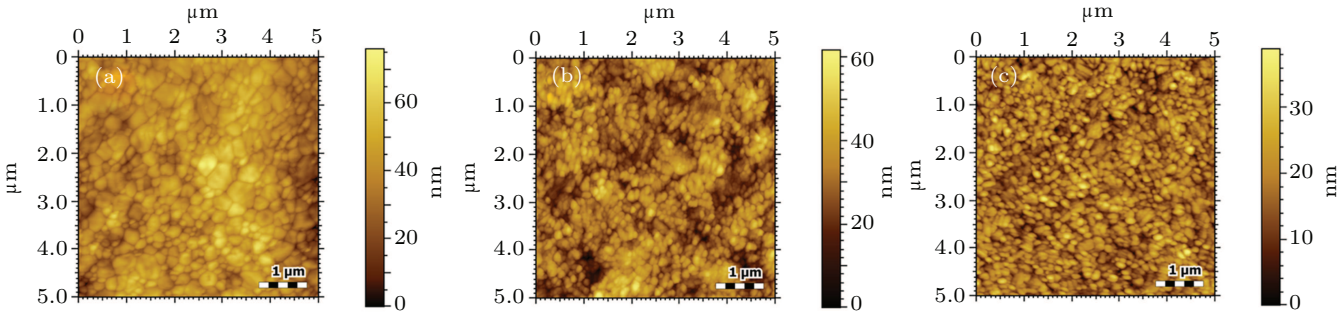


Fig. 7. AFM images of (a) FTO/SnO_2/perovskite, (b) FTO/SnO_2/perovskite/$NiEt_2Pc$, and (c) FTO/SnO_2/perovskite/$NiPr_2Pc$.

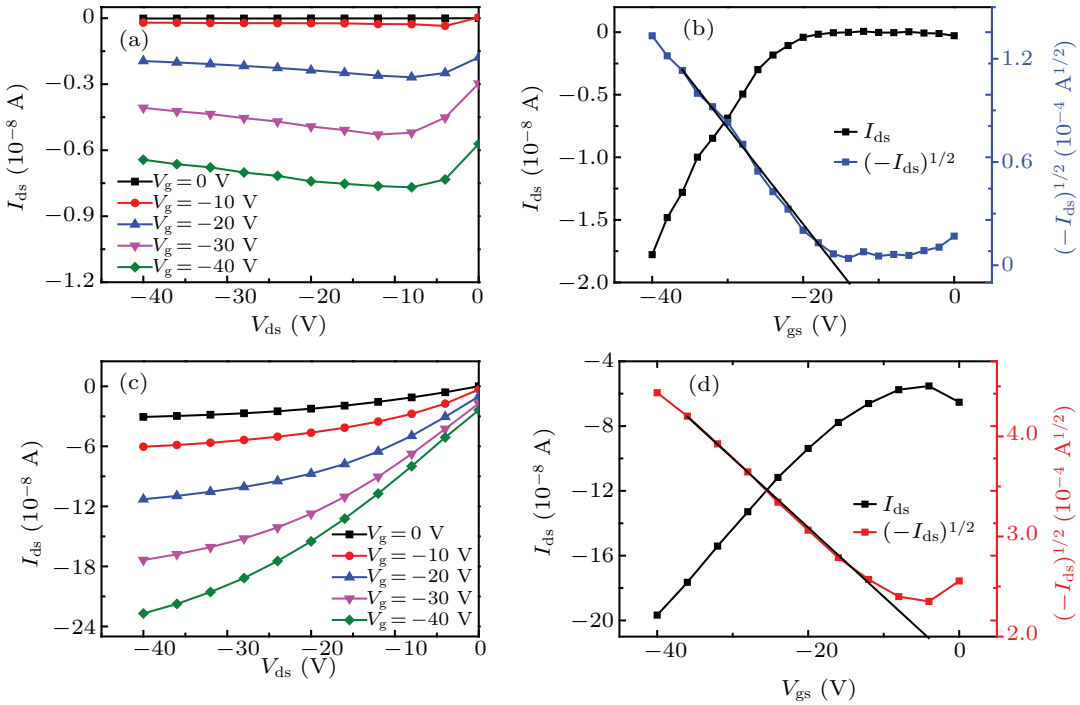


Fig. 8. (a) Output and (b) transfer curves of bottom-contact FET based on $NiEt_2Pc$, and (c) output and (d) transfer curves of bottom-contact FET based on $NiPr_2Pc$ ($L = 10$ μm, $W = 1500$ μm).

The hole extraction ability of the $NiEt_2Pc$ and $NiPr_2Pc$ HTLs was investigated *via* steady-state photoluminescence (PL) spectra. The PL spectra of the perovskite layers coated with or without HTLs were characterized, as shown in Fig. 9(a). A strong PL signal appearing at ~774 nm is found for the bare perovskite layer, which is induced by the recombination between the photo-generated charge carriers within the perovskite layer.[1,12] The PL spectra was significantly quenched when the perovskite absorber was covered with $NiEt_2Pc$ and $NiPr_2Pc$ layers indicative of efficient separation of photo-induced excitons, as well as efficient hole transport from the perovskite layer to the HTLs.[9,12,15,31] A higher quenching efficiency of 96.5% is observed for the $NiPr_2Pc$/perovskite sample compared with that of the $NiEt_2Pc$/perovskite one (95.5%), indicative of better hole extraction ability of the $NiPr_2Pc$ HTL. To further explore the quenching process, the measurement of time-resolved photoluminescence (TRPL) spectra was performed, as illustrated in Fig. 9(b). The PL decay lifetimes extracted from the TRPL spectra were found to be 71.647, 33.550, and 8.017 ns for the bare perovskite the $NiEt_2Pc$/perovskite and $NiPr_2Pc$/perovskite samples, respectively. Shorter PL decay lifetime observed for the $NiPr_2Pc$/perovskite sample further confirms the superior hole extraction ability of the $NiPr_2Pc$ HTL,[16,31,34] and the results are in good agreement with the J_{SC} values observed for the studied PSCs (Fig. 4, Table 1).

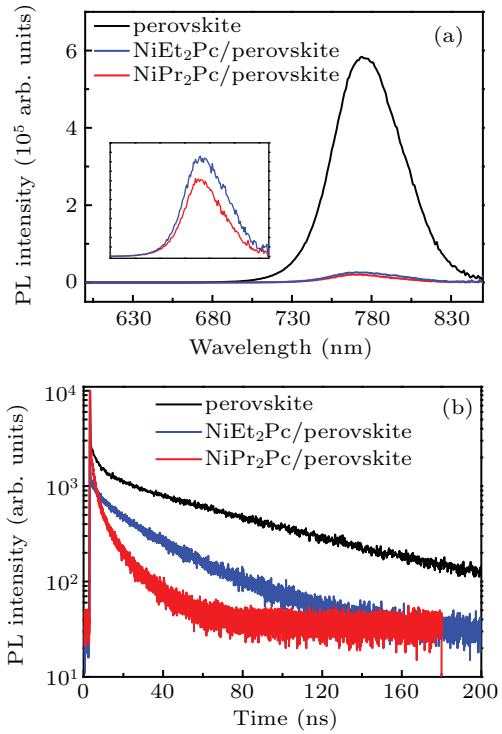


Fig. 9. (a) Steady-state and (b) time resolved PL spectra of bare perovskite, $NiEt_2Pc$/perovskite, and $NiPr_2Pc$/perovskite. The inset in panel (a) is the enlarged steady-state PL spectra of $NiEt_2Pc$/perovskite and $NiPr_2Pc$/perovskite.

4. Conclusions

In summary, two non-peripherally octaethyl- and octapropyl-substituted NiPcs, *i.e.*, $NiEt_2Pc$ and $NiPr_2Pc$, were successfully synthesized and characterized. Both the NiPcs exhibited efficient hole extraction and transport properties when used as dopant-free HTMs in PSCs. The length extension of the alkyl chains from ethyl to propyl significantly increased the NiPcs' LUMO level, which effectively reduced charge carrier recombination at the perovskite/HTL interface, leading to reduced V_{OC} loss and enhanced J_{SC} and FF for the $NiPr_2Pc$-based device. Also, the alkyl chain extension significantly increased hole carrier mobility and affected the crystallinity and surface roughness of thin film, resulting in enhanced hole extraction and transport ability of the $NiPr_2Pc$ HTL. As a result, the $NiPr_2Pc$-based PSC exhibited better device performances than those of the $NiEt_2Pc$-based device.

References

[1] Li C, Hu Q K, Chen Q, Yu W J, Xu J J and Xu Z X 2021 *Org. Electron.* **88** 106018
[2] Kabir I and Mahmood S A 2019 *Chin. Phys. B* **28** 128801
[3] Tian J Li H Wang H Zheng B Xue Y Liu X 2018 *Chin. Phys. B* **27** 18810
[4] Kojima A, Teshima K, Shirai Y and Miyasaka T 2009 *J. Am. Chem. Soc.* **131** 6050
[5] Tu Y, Wu J, Xu G, Yang X, Cai R, Gong Q, Zhu R and Huang W 2021 *Adv. Mater.* **33** 2006545
[6] Bakr Z H, Wali Q, Fakharuddin A, Schmidt-Mende L, Brown T M and Jose R 2017 *Nano Energy* **34** 271
[7] Ameen S, Rub M A, Kosa S A, Alamry K A, Akhtar M S, Shin H S, Seo H K, Asiri A M and Nazeeruddin M K 2016 *ChemSusChem* **9** 10
[8] Rezaee E, Liu X, Hu Q, Dong L, Chen Q, Pan J H and Xu Z X 2018 *Solar RRL* **2** 1800200
[9] Yang G, Wang Y L, Xu J J, Lei H W, Chen C, Shan H Q, Liu X Y, Xu Z X and Fang G J 2017 *Nano Energy* **31** 322
[10] Jiang Q, Zhao Y, Zhang X, Yang X, Chen Y, Chu Z, Ye Q, Li X, Yin Z and You J 2019 *Nat. Photon.* **13** 460
[11] Reddy G, Devulapally K, Islavath N and Giribabu L 2019 *Chem. Rec.* **19** 2157
[12] Wang Y, Ye W, Yang X, Rezaee E, Shan H, Yang S, Cai S, Pan J H, Xu J and Xu Z X 2020 *Synth. Met.* **259** 116248
[13] Seo J, Jeon N J, Yang W S, Shin H W, Ahn T K, Lee J, Noh J H and Seok S I 2015 *Adv. Energ. Mater.* **5** 1501320
[14] Dao Q D, Fujii A, Tsuji R, Takeoka Y and Ozaki M 2017 *Org. Electron.* **43** 156
[15] Wang Y, Liu X, Shan H, Chen Q, Liu T, Sun X, Ma D, Zhang Z, Xu J and Xu Z X 2017 *Dyes Pigm.* **139** 619
[16] Feng Y, Hu Q, Rezaee E, Li M, Xu Z X, Lorenzoni A, Mercuri F and Muccini M 2019 *Adv. Energy Mater.* **9** 1901019
[17] Xu H, Chen R, Sun Q, Lai W, Su Q, Huang W and Liu X 2014 *Chem. Soc. Rev.* **43** 3259
[18] Shan H, Wang Y, Li C, Hu Q, Sun X, Dong L, Feng Y, Ye W, Xu J and Xu Z X 2018 *Org. Electron.* **58** 197
[19] Wang Y L, Shan H Q, Sun X Z, Dong L, Feng Y M, Hu Q K, Ye W K, Roy V A L, Xu J J and Xu Z X 2018 *Org. Electron.* **55** 15
[20] Zheng L P, Xu J J, Feng Y M, Shan H Q, Fang G J and Xu Z X 2018 *J. Mater. Chem. C* **6** 11471
[21] Chen Q, Yang S, Dong L, Cai S, Xu J and Xu Z 2019 *Chin. Phys. B* **29** 017302
[22] Hu Q, Rezaee E, Dong L, Dong Q, Shan H, Chen Q, Li M, Cai S, Wang L and Xu Z X *Solar RRL* **0** 1900182
[23] Xu J J, Wang Y L, Shan H Q, Lin Y W, Chen Q, Roy V A L and Xu Z X 2016 *ACS Appl. Mater. Interfaces* **8** 18991

[24] Xu J J, Wang Y L, Chen Q, Lin Y W, Shan H Q, Roy V A L and Xu Z X 2016 *J. Mater. Chem. C* **4** 7377
[25] Xu Z X, Roy V A L, Low K H and Che C M 2011 *Chem. Commun.* **47** 9654
[26] Hu Q, Rezaee E, Dong Q, Shan H, Chen Q, Wang L, Liu B, Pan J H and Xu Z X 2019 *Solar RRL* **3** 1800264
[27] Ghani F, Kristen J and Riegler H 2012 *J. Chem. Eng. Data* **57** 439
[28] Hu Q, Rezaee E, Li M, Chen Q, Cao Y, Mayukh M, McGrath D V and Xu Z X 2019 *ACS Appl. Mater. Interfaces* **11** 36535
[29] Wang Y, Zheng X, Liu X, Feng Y, Shan H, Dong L, Fang G and Xu Z X 2018 *Org. Electron.* **56** 276
[30] Zheng X, Wang Y, Hu J, Yang G, Guo Z, Xia J, Xu Z and Fang G 2017 *J. Mater. Chem. A* **5** 24416
[31] Liu X, Wang Y, Rezaee E, Chen Q, Feng Y, Sun X, Dong L, Hu Q, Li C and Xu Z X 2018 *Solar RRL* **2** 1800050
[32] Zhang C, Lu Y N, Wu W Q and Wang L 2021 *Nano Energy* **81** 105634
[33] Wetzelaer G J A H, Scheepers M, Sempere A M, Momblona C, Ávila J and Bolink H J 2015 *Adv. Mater.* **27** 1837
[34] Qin P L, He Q, Chen C, Zheng X L, Yang G, Tao H, Xiong L B, Xiong L, Li G and Fang G J 2017 *Solar RRL* **1** 1700058